Exp. Anim. 68(1), 35–47, 2019

—Original—

Rabbit induced pluripotent stem cells retain capability of *in vitro* cardiac differentiation

Praopilas PHAKDEEDINDAN[1)], Piyathip SETTHAWONG[2)], Narong TIPTANAVATTANA[3)], Sasitorn RUNGARUNLERT[4)], Praewphan INGRUNGRUANGLERT[5)], Nipan ISRASENA[5)], Mongkol TECHAKUMPHU[2)] and Theerawat THARASANIT[2,6)]

[1)]*Biochemistry Unit, Department of Physiology, Faculty of Veterinary Science, Chulalongkorn University, 39 Henri-Dunant Rd., Pathumwan, Bangkok 10330, Thailand*
[2)]*Department of Obstetrics, Gynaecology and Reproduction, Faculty of Veterinary Science, Chulalongkorn University, 39 Henri-Dunant Rd., Pathumwan, Bangkok 10330, Thailand*
[3)]*Faculty of Veterinary Science, Prince of Songkla University, 15 Kanjanavanich Road, Hat Yai Songkhla 90110, Thailand*
[4)]*Faculty of Veterinary Science, Mahidol University, 999 Phutthamonthon Sai 4 Road, Nakhonpathom, 73170, Thailand*
[5)]*Stem cells and Cell therapy research unit, Faculty of Medicine, Chulalongkorn University, 1873 Henri-Dunant Rd., Pathumwan, Bangkok 10330, Thailand*
[6)]*The Research and Development Center for Livestock Production Technology at the Faculty of Veterinary Science, Chulalongkorn University, Thailand*

Abstract: Stem cells are promising cell source for treatment of multiple diseases as well as myocardial infarction. Rabbit model has essentially used for cardiovascular diseases and regeneration but information on establishment of induced pluripotent stem cells (iPSCs) and differentiation potential is fairly limited. In addition, there is no report of cardiac differentiation from iPSCs in the rabbit model. In this study, we generated rabbit iPSCs by reprogramming rabbit fibroblasts using the 4 transcription factors **(***OCT3/4, SOX2, KLF4, and c-Myc*). Three iPSC lines were established. The iPSCs from all cell lines expressed genes (*OCT3/4, SOX2, KLF4 and NANOG*) and proteins (alkaline phosphatase, OCT-3/4 and SSEA-4) essentially described for pluripotency (*in vivo* and *in vitro* differentiation). Furthermore, they also had ability to form embryoid body (EB) resulting in three-germ layer differentiation. However, ability of particular cell lines and cell numbers at seeding markedly influenced on EB formation and also their diameters. The cell density at 20,000 cells per EB was selected for cardiac differentiation. After plating, the EBs attached and cardiac-like beating areas were seen as soon as 11 days of culture. The differentiated cells expressed cardiac progenitor marker FLK1 (51 ± 1.48%) on day 5 and cardiac troponin-T protein (10.29 ± 1.37%) on day 14. Other cardiac marker genes (cardiac ryanodine receptors *(RYR2),* α-actinin and *PECAM1*) were also expressed. This study concluded that rabbit iPSCs remained their *in vitro* pluripotency with capability of differentiation into mature-phenotype cardiomyocytes. However, the efficiency of cardiac differentiation is still restricted.
Key words: BMP4, cardiac differentiation, iPSC, rabbit, stem cells

(Received 7 May 2018 / Accepted 10 July 2018 / Published online in J-STAGE 8 August 2018)
Address corresponding: T. Tharasanit. e-mail: Theerawat.t@chula.ac.th
Supplementary data: Video of rhythmic beating area derived rabbit iPSCs can be found online at http://dx.doi.org/10.17632/5n3dgm5bs5.1

Introduction

Induced pluripotent stem cells (iPSCs) as well as embryonic stem (ES) cells are pluripotent stem cells that have unlimited self-renewal and capability to differentiate into all three germ layers and their derivatives [44]. The iPSCs are expected cell source for cell replacement therapy in several diseases including cardiac malfunction. Successful transplantation of cardiomyocyte-like cells derived from iPSCs has been demonstrated to improve cardiac structure and electrophysiological functions in small rodent models [25, 31]. These rat models, however, have short lifespan and different cardio-physiology comparing with human. Therefore, translational knowledge from these species to human application is rather difficult [37]. Rabbit is middle-sized animal model that is commonly used to study cardiovascular diseases, especially atherosclerosis and myocardial abnormalities as molecular mechanisms in cardiac diseases are closely similar to human [9, 38]. However, information on generation of rabbit iPSCs has been limited as only few laboratories have demonstrated the possibility on establishment of rabbit iPSCs. In addition, there is no information on *in vitro* cardiac differentiation in rabbit. BMP4 has been used to promote differentiation of pluripotent stem cells into cardiac cell lineage [22]. The BMP4 induces mesoderm formation via ERK pathway and up-regulates the mesoderm markers (*Brachyury* and Fetal liver kinase 1) [3, 22]. Fetal liver kinase 1 (FLK1), an early receptor tyrosine kinase, is useful surface marker for determining mesodermal cells [8, 12, 30, 50]. FLK^+ cells derived from pluripotent cells could develop into cardiomyocyte, hematopoietic and endothelial cells [19, 21, 32, 35]. Furthermore, the BMP4 also promotes gene expressions of cardiac progenitors (*NKX2.5* and *GATA4*) [43] and enhances cardiac differentiation via MAP kinase, Tak1 and Smad family [1, 26]. The action of BMP4 to drive mesodermal differentiation of cardiac lineage can be efficiently promoted by three-dimension cell aggregation via embryoid body (EB) formation [23]. It has been reported in mouse that relatively large EB size (around 450 μm) promoted cardiac differentiation better than smaller size EB (150 μm) [17]. However, the effects of cell seeding density and EB size in relation to cellular aggregation (EB formation) and cardiac differentiation have yet to be studied in rabbit model. In this study, we aimed at establishing induced pluripotent stem cells in rabbit and examined *in vitro* differentiation of rabbit iPSCs toward cardiac lineage.

Materials and Methods

Reagents and animals

All chemicals were purchased from Invitrogen Life Technologies (Carlsbad, CA, USA), otherwise indicated. ICR mice and New Zealand White rabbits were purchased from the National Laboratory Animal Center (Mahidol University, Thailand). BALB/c nude mice were purchased from Nomura Siam International Co., Ltd. (Bangkok, Thailand). Animal maintenance, care, and use procedures were performed according to the Animal Ethics Approval of Chulalongkorn University (No.1673036).

Generation of rabbit induced pluripotent stem cells

The plasmids for retrovirus vectors were purchased from Addgene (www.addgene.com); pMXs-hOCT3/4 (Cat# 17217), pMXs-hSOX2 (Cat# 17218), pMXs-hKLF4 (Cat# 17219) and pMXs-hc-MYC (Cat# 17220). The virus was produced using pMXs-vector (16 μg) and pVSV-G (4 μg) in 293GP cells by X-tremeGENE Reagents (Roche, Mannheim, Germany) according to manufacturer's instructions. Rabbit embryonic fibroblasts (REF) were transfected twice with retrovirus in the presence of 4 μg/ml polybrene (Sigma Aldrich, WI, USA). The transfected REF were dissociated and seeded at a density of 1,000 cells per cm^2 on mitomycin inactivated MEFs (mouse embryonic fibroblast). The iPSC medium was composed of DMEM/F12 containing 20% (v/v) KnockOut serum replacement (KSR), 1 mM L-glutamine, 1% (v/v) non-essential amino acids (NEAA), 0.1 mM β-mercaptoethanol, 1,000 IU/ml Leukemia inhibitory factor (LIF, Millipore, CA, USA) and 10 ng/ml basic fibroblast growth factor (bFGF, R&D Systems, MN, USA). The induced pluripotent stem (iPS) cell-like colonies were observed on day 7–21 post-transduction. The iPS primary colonies were examined under a phase contrast microscope (Olympus, Shinjuku, Japan). The iPSCs were continuously subcultured by enzyme (Tryple™ Select). In all cases, culture condition was performed at 37°C in a humidified condition of 5% CO_2 in atmosphere. To determinate of reprogramming efficiency (RE), transfected REF were passaged and seeded at a density of 600 cells/cm^2. Total primary colonies (larger than 100 μm) were examined for alkaline phosphatase (ALP) activity and counted on day 7 after reprograming.

Table 1. Primers used in polymerase chain reaction (PCR) in this study

	Forward (5'–3')	Reverse (5'–3')	Product size (bps)	Tm	Accession number or reference
OCT3/4	CCTTCGCAGGGGGGCCTA	CATGGGGGAGCCCAGAGCA	161	55	[15]
NANOG	CACTGATGCCCGTGGTGCCC	AGCGGAGAGGCGGTGTCTGT	94	60	[36]
SOX-2	AGCATGATGCAGGAGCAG	GGAGTGGGAGGAAGAGGT	270	55	XM_008266557.2
KLF4	TCCGGCAGGTGCCCCGAATA	CTCCGCCGCTCTCCAGGTCT	131	55	[36]
hOCT3/4	GTTGCTCTCCACCCCGACTCCTGCTTC	GAGAACCGAGTGAGAGGCAAC	376	60	[5]
hSOX2	CCAGATCCCGCACAAGAGTT	CAAGAGGCGAACACACAACG	264	60	[44]
hKLF4	GGCTGATGGGCAAGTTCG	CTGATCGGGCAGGAAGGAT	416	60	[5]
hc-Myc	GCAGCGACTCTGAGGAGGAACAA	TTTTCCTTACGCACAAGAGTTCCGT	581	60	[5]
GBX2	AACGCGTGAAGGCGGGCAAT	TGCTGGTGCTGGCTCCGAAT	118	55	[36]
PAX6	GAACAGACACAGCCCTCACA	TCGTAACTCCGCCCATTCAC	160	55	NM_001082217.1
PITX2	AACCTTACAGAAGCCCGAGT	GGAAACTCTTGGTGGACAGC	217	55	XM_008267481.1
CFTR	CACAATTGAAAGCAGGTGGGA	GTTGCTGTGAGGTATGGAGG	225	55	NM_001082716.1
PECAM1	AGAGGAGCTGGAGCAGGTGTTAAT	GCTGATGTGGAACTTCGGAACAGA	145	55	[36]
α-actinin	CCATATAAGCTGGAAGGACG	GTACTTCTCTGCCACATCAA	139	55	XM_002719521.3
RYR2	GAGCAACGGAGGACTGTTCA	TGACGTAGTCGGAATGGCTG	134	55	NM_001082757.1
GAPDH	TGGTGAAGGTCGGAGTGAAC	ATGTAGTGGAGGTCAATGAATGG	121	55	NM_001082253.1

RE was calculated by the following formula.

$$RE = \frac{primary\ colonies \times 100}{total\ of\ transfected\ seeding\ cells}$$

To evaluate the percentage of rabbit iPSC line establishment (% riPSCL). Ten colonies derived transfected REF were selected randomly for iPSC establishment and characterization. % riPSCL was calculated by the following formula.

$$\%\ riPSCL = \frac{a\ number\ of\ cell\ lines \times 100}{a\ number\ of\ selected\ colonies}$$

Karyotyping and G-banding

Rabbit iPSCs were disassociated and centrifuged at 200 × *g* for 5 min. The cell pellet was incubated at 37°C for 20 min in 0.075 M KCl. The cells were washed twice and fixed with a mixture of acetic and methanol (1:3) on ice. They were dropped vertically onto a glass slides and stained with 10% (v/v) Giemsa solution. Numbers of chromosome from at least 20 metaphase spreads were evaluated under a light microscope. For g-banding, the slides containing metaphase spreads were aged for at least 1 week, then the chromosomes were partially digested with 0.05% Trypsin-EDTA, stained with Giemsa and analyzed under a light microscope.

Reverse transcriptase polymerase chain reaction (RT-PCR)

REF, rabbit iPSCs and differentiated cells were sampled and stored at −80°C prior to analysis. RNA was extracted using an RNeasy Mini Kit (Qiagen). The amount of RNA and purity were measured by Nanodrop 2000 spectrophotometer (ThermoFisher Scientific, DE, USA). DNase I (Promega, WI, USA) was used to eliminate contaminated DNA. cDNA synthesis (RT+) was performed using SuperScript III Kit (Invitrogen) according to the manufacturer's instructions. Negative control was performed as described above without superscript III reagents (RT−). cDNA was performed using the specific primers listed in Table 1. The PCR cycles were as follows: initialization at 95°C for 2 min, followed by 30 PCR cycles of denaturation at 95°C for 30 s, annealing step at 55–64°C for 30 s and extension step at 72°C for 30 s. To determine the downregulation, the presence of exogenous genes (*hOCT3/4, hKLF4, hSOX2* and *hc-Myc*) was investigated in REF and rabbit iPSC line R1, R2 and R3 at passage 17 using RT-PCR analysis. This was performed simultaneously with the expression of endogenously rabbit pluripotent genes (*OCT3/4* and *NANOG*). Mixture of extracted plasmid (pMXs-hOCT3/4, pMXs-hSOX2, pMXs-hKLF4 and pMXs-hc-MYC) were served as positive control in study of exogenous expression.

Alkaline phosphatase and immunofluorescent staining

The cells were washed with phosphate buffered saline (PBS) and then fixed with 4% (w/v) paraformaldehyde (PFA) for 15 min. Alkaline phosphatase (ALP) activity was tested using Alkaline Phosphatase Kit (Sigma-Aldrich, MO, USA) following the manufacturer's instructions. The pink-to-red colored colonies were classified as positive to ALP activity. To investigate protein expression, the cells were passaged onto a cover slip and then

fixed with 4% (w/v) PFA. The cells were permeabilized if necessary in mixture of 0.1% Triton X-100, 2% bovine serum albumin (BSA) in PBS and the non-specific binding was blocked with 2% BSA. The cells were incubated at 4°C with primary antibodies overnight. The primary antibodies in this study included OCT-3/4 (SC8628, Santa Cruz Biotechnology, TX, USA , 1:100), SSEA-4 (ab16287, Abcam, Cambridge, UK , 1:50), FLK1 (SC393163, Santa Cruz Biotechnology, 1:100) and cTnT (troponin T, ab33589, Abcam, 1:100). The samples were then stained with secondary antibody corresponding to the primary antibodies used. The 4', 6'-diamidino-2-phenylindole (DAPI) in mounting medium (VECTASHIELD® Mounting Medium, Vector Laboratories, CA, USA) was used to visualize the nucleus. The negative control was performed as described above without primary antibody. A fluorescent microscope (BX51, Olympus) and DP2-BSW software were used for visualization and record the samples.

In vitro differentiation

Differentiation was performed using a hanging drop technique in order to promote cell aggregation into three-dimension structure referred as embryoid bodies (EBs). The iPSC lines R1, R2 and R3 (passage 22–25) were dissociated and seeded in each culture drop (20 μl) at the density 20,000 cells in DMEM/F12 medium containing 15% (v/v) FBS. To examine the *in vitro* differentiation, there different techniques were used. Firstly, we investigated the presence of endogenously pluripotent genes (*OCT3/4, NANOG, KLF4* and *SOX2*) in the cell lines after EB formation for 2 and 7 days. Secondly, gene expressions of three-germ differentiation were additionally examined on day 7 of EB plating using RT-PCR. These included the expressions of ectoderm (*PAX6* and *GBX2*), mesoderm (*PECAM1*) and endoderm (*PITX2* and *CFTR*). The presence of proteins associated with three-germ layer differentiation was demonstrated by immunohistochemistry (Leica Microsystems BOND-MAX System). In brief, the EBs (day 14 of culture) were fixed with 4% (w/v) PFA. They were embedded in paraffin and cut at a thickness of 4 μm. The slides were incubated with Bond Dewax Solution (Leica Microsystems) for 60 min at 60°C. The epitopes of the antigens were retrieved with Bond Epitope Retrieval Solution 2 (Leica Microsystems) for 30 min at 100°C. The slides were separately incubated with primary antibodies including mouse monoclonal anti-glial fibrillary acidic protein (anti- GFAP, 6F2, DAKO, 1:2,400), anti-Vimentin (V9, CellMarque, CA, USA , 1:400) and anti-β-catenin (14, CellMarque, CA, USA , 1:500) at 25°C for 40 min and followed by 3 consecutive rinses with a Bond Wash Solution (Leica Microsystems). Hydrogen peroxide (3%) was then applied for 5 min and rinsed 3 times. Post primary polymer (Leica Microsystems) were applied for 8 min. The slides were washed, followed with Poly-HRP IgG (Leica Microsystems) for 8 min, and rinsed 3 times. The diaminobenzidine chromogen was applied for 4 min followed by 3 deionized water rinses. Slides were counterstained with hematoxylin for 5 min. Isotype Mouse IgG1, kappa monoclonal (ab91353, Abcam, Cambridge, UK) were used instead of the primary antibody for the negative control. Brain tumor, appendix and tonsil were used as positive controls for GFAP, vimentin and β-catenin, respectively.

Teratoma formation

To generate teratomas, 5×10^6 of rabbit iPSC lines (R2 and R3 passage 22) were subcutaneously injected into six 8-week-old BALB/c nude mice (3 mice per cell line). Around 6–8 weeks after transplantation, the teratomas were observed and dissected. The masses were fixed in 4% (w/v) PFA. The samples were embedded in paraffin and cut at a thickness of 4 μm. The samples were deparaffinized and stained with hematoxylin and eosin (HE staining). The slides were examined under a light microscope by an experienced pathologist.

Cardiac differentiation

The protocol for cardiac differentiation via hanging drop technique was performed as previously described [42] with minor modification. Briefly, iPSC lines R1, R2 and R3 (passage 22–25) were dissociated and allowed to aggregate into three-dimension in EB medium which was composed of DMEM/F12 medium supplemented 1 mM L-glutamine, 1% (v/v) NEAA, 0.1 mM β-mercaptoethanol, BMP4 (10 ng/ml) and 15% (v/v) FBS (HyClone™, Utah, USA). To optimize for cardiac differentiation, hanging drop technique was performed using different cell density of 1,000, 3,000, 5,000, 10,000 and 20,000 cells per droplet (day 0). The EBs were harvested from hanging drop on day 2 and cultured as suspension. An Olympus CKX41 inverted microscope was used for phase-contrast imaging of EBs at 72 h post EB culture. The cross-sectional diameters of EBs were measured by ImageJ (https://imagej.nih.gov/ij/). For further

examination of cardiac differentiation, optimal starting cell seeding density were selected. Hanging drop was performed with EB medium combined BMP4 treatment. The EB were harvested from hanging drop into suspension with 10 ng/ml BMP4 treatment on day 2. On day 3, the EBs were further plated onto gelatin coated dishes or coverslips with EB medium without BMP4. On day 5 of differentiation, the plating EB on gelatin were digested using TrypLE^{TM} Select (1X) into small clump or single cells, and the cells were counted for cardiovascular progenitor surface marker, FLK1. The proportion of FLK1 positive cells were evaluated by the number of cells positive to FLK1 in relation to the total cell numbers (at least 100 cells, three independent experiments of each cell line). To study mature cardiomyocyte marker (cTnT) plating EB on day 14 of iPSC cell lines R1, R2 and R3 were used. The plating EB on gelatin coated dishes were digested were counted for cardiomyocyte marker cTnT (at least 100 cells, four independent experiments of each cell line). The immunolabeling for FLK1 and cTnT was performed as previously described. The cells positive cTnT on coverslips were photographed using a fluorescent microscope (BX51, Olympus) and DP2-BSW software. In addition, cardiac gene (cardiac ryanodine receptors (*RYR2*), α-actinin and *PECAM1*) were studied in all cell lines using the same protocols. Briefly, the plating EB on day 14 were mechanically harvest form gelatin coated dishes. The mRNA was extracted and RT-PCR analysis were performed as previously described. The differentiated cells were observed daily and the remaining of differentiated cells besides harvested samples in all experiments were observed for cardiac beating area until day 21. The medium was changed in plating EB every 2–3 days until harvest.

Statistical analysis

Data of EB diameters are represented as mean ± SD. Data for FLK1 and cTnT positive cells are represented as mean ± SEM. The statistical differences among experimental groups were analyzed by one-way Analysis of Variance and Tukey's Multiple Comparison Test analysis using GraphPad Prism (www.graphpad.com). *P* value less than 0.05 ($P<0.05$) was considered statistically significant.

Results

Several primary colonies were observed as soon as 4 days post transfection. The reprogramming efficiency calculating from number of transfected fibroblasts that gave rise to ALP positive colonies was 0.191%. Three cell lines were established (referred to as R1, R2 and R3 cell lines) and the percentage of riPSCL was 30%. These cell lines maintained ES-like morphology with positive ALP staining for over 35 passages without losing their proliferative activity. Rabbit iPSC colonies demonstrated distinct boundary between the colonies and feeder cells (Fig. 1A). The colonies contained iPSCs having high nuclear per cytoplasm ratio and prominent nucleoli. The colonies were strongly positive to ALP (Fig. 1B) and to OCT-3/4 and SSEA-4 proteins (Figs. 1C and D). RT-PCR also indicated that they endogenously expressed pluripotent genes (*OCT3/4, SOX2, KLF4* and *NANOG*, Fig. 1F). Karyotyping and G-banding analysis revealed that the cell lines had normal chromosome numbers (n=44, Fig. 1G). Human exogenous genes (*hOCT3/4, hKLF4, hSOX2* and *hc-Myc*) were absent in all rabbit iPSC cell lines (R1, R2, and R3), while the endogenous pluripotent genes *OCT3/4* and *NANOG* were presented (Fig. 1E). All rabbit iPSC lines could form 3-dimension structure by mean of embryoid body formation (Fig. 2A). This property of the rabbit iPSC cell lines coincided with the down regulation of pluripotent genes (*OCT3/4, NANOG, KLF4* and *SOX2*). *NANOG* expression was completely downregulated by day 2 of EB formation, while *KLF4*, *SOX2* and *OCT3/4* were still expressed (Fig. 2C). Although *KLF4 and SOX2* genes were continuously expressed on day 7 of EB culture, the expression of *OCT3/4* gene was abolished at this time point. Simultaneously, the EB culture led to the differentiation of rabbit iPS cells indicating by the expressions of ectodermal (*GBX2, PAX6*), mesodermal (*PECAM1*) and endodermal markers (*PITX2, CFTR*) (Fig. 2B). Furthermore, the culture of EBs for 14 days also resulted in the differentiation of the iPS cells into three-germ layer structure as shown in Fig. 2D. The immunohistochemistry of EBs revealed the presences of protein expressions of ectoderm (GFAP), mesoderm (Vimentin) and endoderm (β-catenin) markers in all cell lines (Fig. 2D).

Two rabbit iPS cell lines (R2 and R3) were used to demonstrate the capability of *in vivo* differentiation. These two cell lines were capable of *in vivo* differentiation by mean of teratoma formation after cell transplantation into immunocompromised mice. However, the R3 cell line had greater incidence of teratoma formation (2/3, 66.67%) when compared with the R2 cell line (1/3,

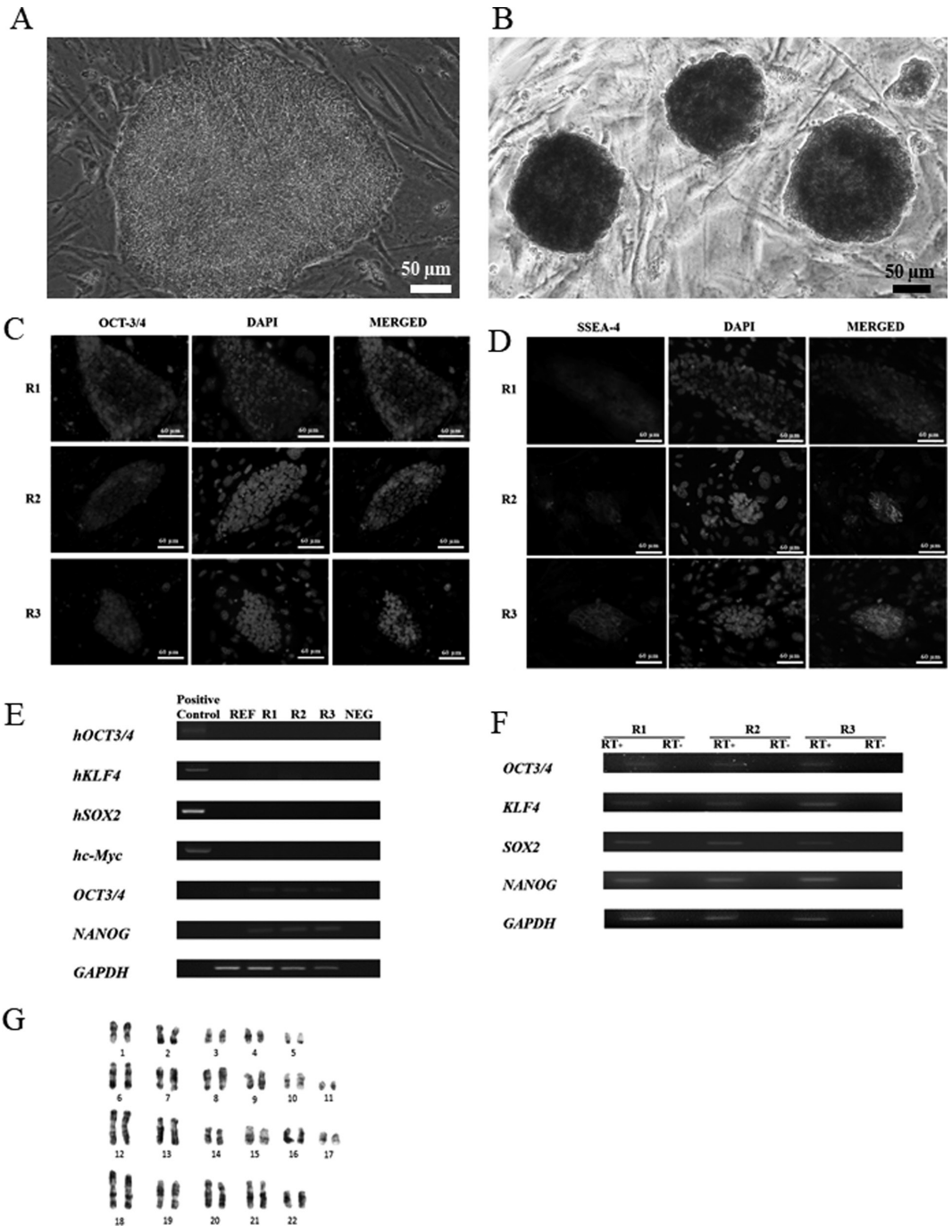

Fig. 1. Characterization of rabbit iPSCs (A) the colony morphology of rabbit iPSC line R3 at passage 18 (B) ALP staining of rabbit iPSC line R3 at passage 18. (C) The rabbit iPSCs were positive stained with OCT-3/4 (green) located in nucleus and co-staining with DAPI (blue). Scale bar represents 60 μm. (D) The rabbit iPSCs were positive stained with stage specific embryonic antigen-4 (SSEA-4) at cell membrane, nucleus were stained with DAPI (blue). Scale bar represents 60 μm. (E) Absence of expression of exogenous pluripotent genes (*hOCT3/4, hSOX2, hKLF4* and *hc-Myc*) in rabbit embryonic fibroblasts (REF) and rabbit iPSC line R1, R2 and R3 at passage 17. Mixture of extracted plasmid were served as positive control. (F) Expression (RT+) of endogenous pluripotent genes (*OCT3/4, SOX2, NANOG* and *KLF4*) in rabbit iPSC line R1, R2 and R3 at passage 22. PCR without superscript III reagents (RT-) was performed as negative control. (G) G-banding of rabbit iPSC R2 at passage 22

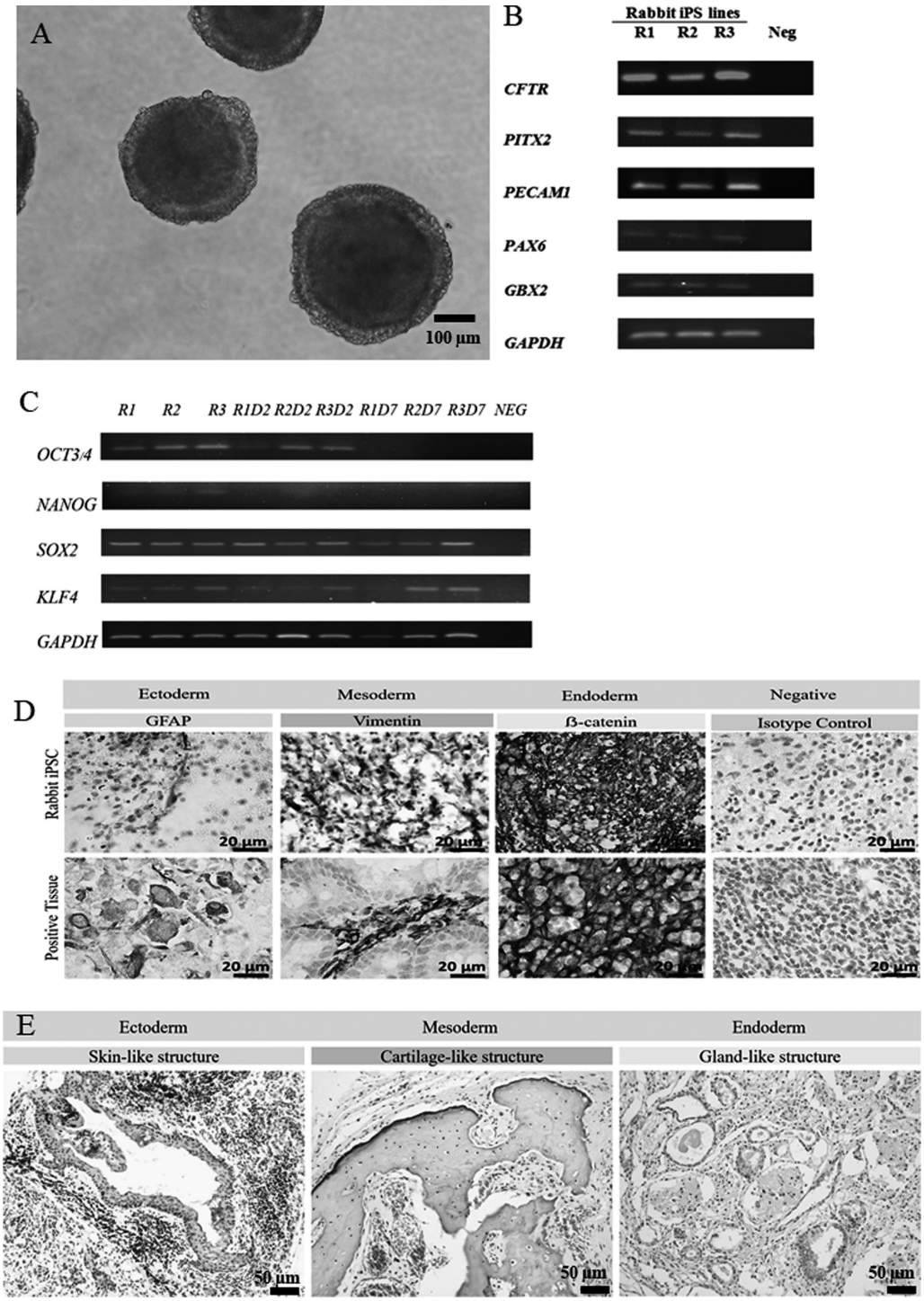

Fig. 2. *In vitro* differentiation in rabbit pluripotent cells. (A) Representative image of embryoid bodies derived from 20,000 cell density starting at day 3 in DMEM/F-12 containing 15% FBS. Scale bar represents 100 μm. (B) Gene expression of three germ layers; *CFTR* and *PITX2* (endoderm), *PECAM1* (mesoderm) and *PAX6* and *GBX2*(ectoderm) in day 7 EBs derived from rabbit iPSC line R1 R2 and R3 at passage 22. (C) Endogenous pluripotent genes in EB day 2 and day7. (D) Day 14 EB were fixed and stained with antibodies against GFAP, vimentin and β-catenin to identify specific cell lineages. Scale bar represent 20 μm. (E) HE staining of teratoma section generated by rabbit iPSCs demonstrated structures derived from three germ layer tissue: epidermis (left panel; ectoderm), cartilage (middle panel; mesoderm) and gland-like structure (right panel; endoderm). Scale bar represent 50 μm.

33.33%). The histological findings after the haematoxylin and eosin staining confirmed the structures of teratoma that derived from three-germ layers of origin including epidermis-like (ectoderm), cartilage-like (mesoderm) and gland-like (endoderm) structures (Fig. 2E).

For cardiac differentiation, all the cell lines could contribute to three-dimensional mass but the ability to form EB was different among the cell seeding densities and particular cell lines. In general, cell seeding density influenced the EB size. Low cell seeding density at 1,000 cells per EB was insufficient to form EB in all cell lines. A cell line (R1) did not form the EB at 3,000 cells/EB (Fig. 3A-1). At 5,000 and 10,000 cell density, iPSC line R2 could form EB with larger size compared with R1 and R3 lines (P<0.05, Figs. 3A-2 and 3). Cell seeding density at 20,000 cells per EB increased EB size to the range of 326 to 467 μm which was previously reported to be optimal EB size for cardiac differentiation [17, 29]. This cell density (20,000 cells per EB) was therefore used for cardiac differentiation in this study. The average diameters of EBs obtained for 20,000 cells/EB were 325.8 ± 7.32, 467.4 ± 8.68 and 463.33 ± 18.42 for iPSC line R1, R2 and R3, respectively. After EBs were cultured for 72 h in the EB medium with BMP4, they were harvested and cultured onto gelatin coated dishes. The EBs were easily attached to the Petridish and cells were translocated from outermost area of the EBs to form multiple cell types and layers. On day 5 of differentiation, a large proportion of cells (51 ± 1.48%) positively expressed with cardiovascular progenitor marker, FLK1 (Figs. 3D-1 and 2). There was no significant difference among cell lines. The mean ± SEM of FLK1 positive cells were 53.33 ± 2.3%, 53.17 ± 1.58% and 46.49 ± 2.5% for iPSC line R1, R2 and R3, respectively. Later, the outer layer contained flat elongated cells while the center remained dense darkened area. The elongated cells were seen around day 7 of cardiac differentiation (Fig. 3B). They formed filament-like structure and started to spontaneously beat around day 11 to 14 of culture (supplementary data). In addition, these cells also expressed cardiac marker genes including *RYR2, PECAM1* and α-actinin (Fig. 3C). For all cell lines, a small proportion of cells were positively stained with cTnT (10.29 ± 1.37%) with striated structure, indicating morphology of mature cardiomyocytes (Fig. 3E). The mean ± SEM of cTnT positive cells in R3 was lowest (4.24 ± 0.16%, P<0.05). There was no significant difference between line R1 (14.45 ± 0.54%) and line R2 (12.19 ± 1.13%).

Discussion

In this study we established rabbit iPSCs and demonstrated that the iPSCs have differentiation potential toward cardiac lineage. Until recently, a limited number of rabbit iPSC lines have been reported [14–16, 36]. However, information on cardiac differentiation of these iPSC lines has not been demonstrated. Rabbit model was a valuable model for cardiac diseases in human [38]. The establishment of iPSC-based therapy for cardiovascular diseases in rabbit model has not yet been established due to the generation of rabbit iPSCs appeared to be difficult and the knowledge on signaling controls of cardiac differentiation is fairly limited. All rabbit iPSC lines including our cell lines were established using viral vectors with ectopic genes *OCT3/4, SOX2, KLF4, and c-Myc* [14, 36, 46]. Although this technique may lead to mutational genome integration [7], this viral transduction is most likely the robust method to introduce ectopic genes into the host genome [41]. In our study, downregulation of human exogenous genes *(hOCT3/4, hKLF4, hSOX2* and *hc-Myc*) was found in all cell lines, simultaneously with the presence of endogenous pluripotent genes *OCT3/4* and *NANOG*. Although the presence of exogenous genes at differentiation may interfere the differentiation process, the poor efficiency of cardiac differentiation therefore appears to involve other factors rather than the existence of the exogenous genes. Our findings are in an agreement to previous reports that the establishment of rabbit iPSCs is very poor [15] and its pluripotency is remarkably limited [16]. The reason for poor results of viral transduction in this species is still unknown but the poor result is similar to previous reports demonstrating an inefficient viral (human immunodeficiency virus) transduction in rabbit cells. This is likely to involve the process of gene transduction at a post-viral entry and pre-integration step [13, 20]. This seems to be species specific since gene transduction efficiency with green fluorescent protein expressing viral vectors into rabbit cells was around 5 to 6 times less efficiency compared to human, feline and porcine fibroblasts (unpublished data). In addition, the maintaining pluripotent factors of rabbit iPSCs are poorly understood. This is critical for establishment of pluripotent cell line as particular species requires different signaling to promote and to sustain their pluripotency pathways. For instance, mouse embryonic stem cells needs to be maintained via LIF/STAT-3 pathway [34] while human ESC mainly

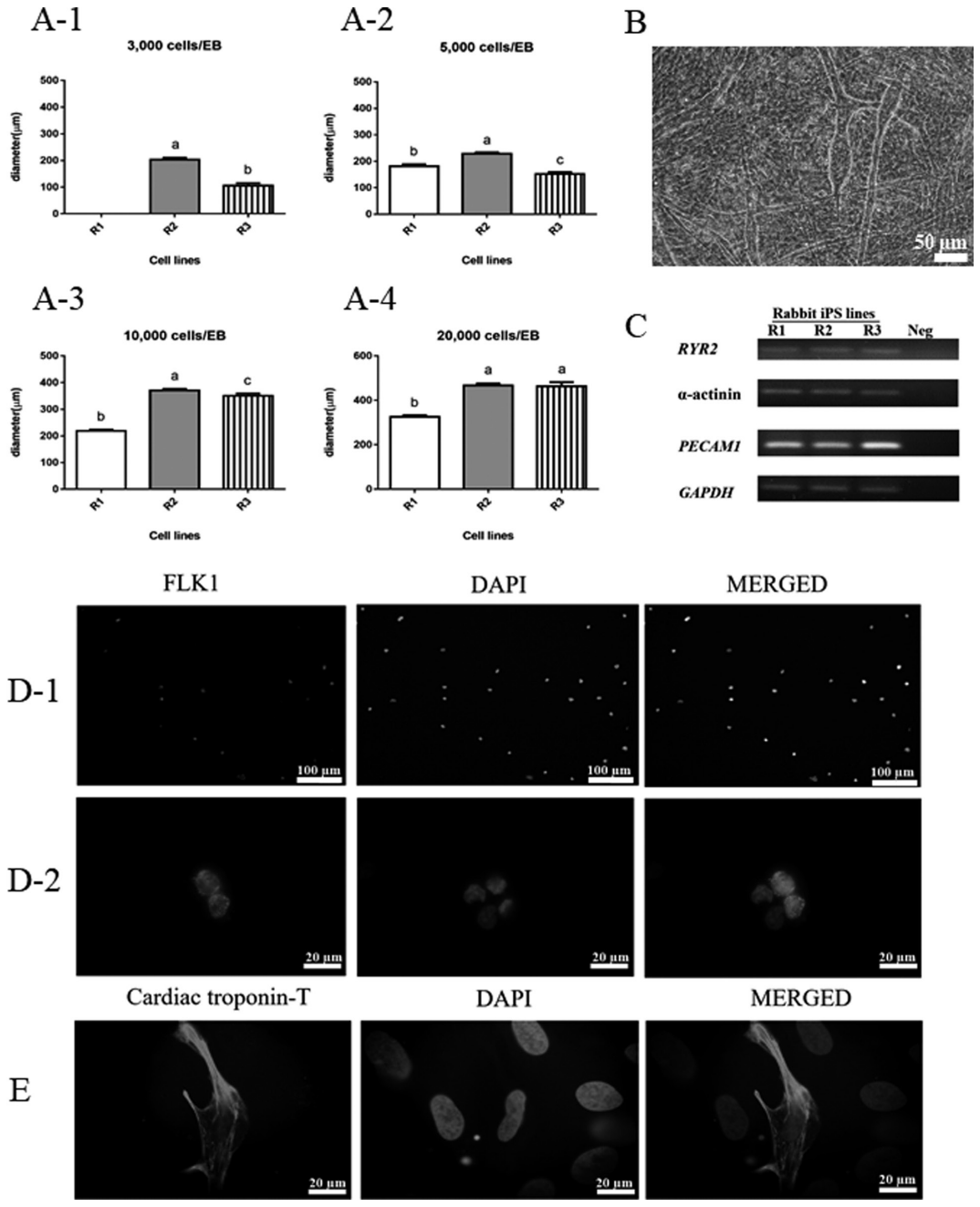

Fig. 3. Cardiac differentiation derived rabbit iPSCs. (A) Analysis of EB diameters at different cell seeding density. *P* value less than 0.05 ($P<0.05$) was considered statistically significant. The graphs were plotted with letter-coded significant differences (a, b, c). (B) Cardiomyocyte-like cells derived iPSCs at day 14. Scale bar represents 50 μm. (C) Gene expression of cardiac markers; cardiac ryanodine receptors (*RYR2*), α-actinin and *PECAM1* in day 14 EBs derived from rabbit iPSC line R1 R2 and R3. (D) Differentiating cells at day 5 were positively stained with mesodermal surface marker FLK1. Scale bar represents 100 μm (D-1) and 20 μm (D-2). (E) Cardiomyocyte-like cells were positively stained with cardiac troponin-T, cTnT. Scale bar represents 20 μm.

requires bFGF for pluripotent maintenance [11, 27]. The rabbit iPSCs established in this study demonstrated typical iPSC morphology (flat colony, Fig. 1A) which is resembled to human iPSCs rather than dome-shaped mouse iPSCs. Furthermore, the findings also are in an agreement with other studies that rabbit iPSCs are LIF

and bFGF dependent [46]. The three cell lines established in the current study had potential to develop into all three germ layers and also cardiac lineage, via cellular aggregation using hanging drop technique. However, we found that the EB culture did not completely downregulate entire pluripotent gene as *SOX2* and *KLF4* genes were found to continuously express on day 7 of EB culture, while the pluripotency controlled *NANOG* and *OCT3/4* genes was completely downregulated. The finding is in an agreement with a report of human embryonic stem cells that *KLF4* could still be detected in the two-week cultured EB [6]. These results suggest that these genes do not only control pluripotency but also balance the cellular homeostasis. For example, the *KLF4* gene has been demonstrated to actively control cellular processes, such as apoptosis [10]. In addition, this study confirmed the capability of retroviral mediated rabbit iPS cell lines in *in vitro* and *in vivo* differentiation, in terms of gene and protein expressions in embryoid body and teratoma formation, respectively. The efficient differentiation appears to associate with the downregulation or silence of exogenous genes used during iPS generation or when the exogenous pluripotent genes were overwhelmed by other pluripotent endogenous genes [33, 40]. In the current study, we differentiated rabbit iPS into cardiac cell fate via embryoid body formation. This technique is simple and has been reported to efficiently promote mesodermal transition and also cardiac differentiation [29, 45], although mature cardiomyocytes can also be generated by other techniques such as monolayer format [28, 51] and direct transdifferentiation [18, 39]. Using this technique, we demonstrated for the first time that the rabbit iPSCs can differentiate toward cardiac lineages (Fig. 3). This capability highlights the possibility to use rabbit as a model for treating cardiac disorder in human. Although all established iPSC lines were capable of forming EBs, this ability was dependent on cell density (cell number per EB) and cell line (Fig. 3C). EB formation was inefficient for low cell density (1,000 and 3,000 cells per EB). This appeared to cause by the sensitivity of rabbit iPSCs on enzymatically single cell dissociation similar to human [2]. We optimized the EB size to around 400 μm since the large EB size (300–450 μm) had been shown to promote cell differentiation into cardiac lineage compared with smaller EBs [17, 29]. The large EB size allowed sufficient cellular interactions and also microenvironments such as oxygen tension suitable for differentiation and proliferation of cardiac progenitor cells [48, 49]. Furthermore, a larger size EB tended to preferentially elevate gene expression (*NKX2.5, GATA4, WNT11, TBX5, NFATC1* and *NRG1*) that are responsible for cardiogenic differentiation [4]. The cardiac differentiation was also promoted by addition of BMP4 during EB formation [22, 45] as the BMP4 is the main regulator for cardiac mesodermal transition and regulates cardiogenesis via NKX2.5 and GATA4 pathways [1, 26]. Although these pathways have not been examined in rabbit iPSCs, the protocol used in this study efficiently differentiated the iPSCs (around 50%) into cardiac progenitor cells by means of FLK1 expression. However, only small population could develop to mature cardiac phenotypes (cTnT positive beating cells). The low efficiency in differentiation of mature cardiac cells may relate to the property of the specific cell lines used. The rabbit iPS cell lines used in this study appears to constantly express *SOX2.* The increased expression of SOX2 potentially guides the cell fate generally into neuroectodermal lineage. This condition inhibits mesodermal differentiation and thereby limiting spontaneous cardiac differentiation [24, 47]. Although BMP4 supplement could improve cardiac differentiation of rabbit iPS cells, over all efficiency remain poor. This suggests that other factors appear to synergistically interact with cardiac cell fate, rather than BMP4 alone. It is interesting to examine whether or not other factors such as activin A, FGF2, VEGF, Gsk3 inhibitors and Dickkopf-1 will be needed for cardiac differentiation as previously reported in human [28, 50]. Further study for improving cardiac differentiation for rabbit iPSCs such as identification of molecular networks for cardiac differentiation should be investigated.

Conclusions

Rabbit iPSC lines can be differentiated into cardiac lineage via 3D-structure embryoid body. The optimization of cardiac differentiation remains to be elucidated in order to improve its efficiency. The findings in this study highlight the possibility to generate mature cardiomyocytes from rabbit iPSCs for further use.

Conflicts of Interest

none.

Acknowledgments

This research was financially supported by National Research Council of Thailand under research scheme "development of cardiomyocyte tissue engineering for treatment of acute ischemic heart: from animal model to personalized human medicine", the Special Task Force for Activating Research (STAR 59-007-31-005) and Mahidol University (E04/2560). Praopilas Phakdeedindan is granted by 100th Anniversary Chulalongkorn University and Overseas Research Experience Scholarship for Graduate Student, Chulalongkorn University.

References

1. Barron, M., Gao, M. and Lough, J. 2000. Requirement for BMP and FGF signaling during cardiogenic induction in non-precardiac mesoderm is specific, transient, and cooperative. *Dev. Dyn.* 218: 383–393. [Medline] [CrossRef]
2. Beers, J., Gulbranson, D.R., George, N., Siniscalchi, L.I., Jones, J., Thomson, J.A. and Chen, G. 2012. Passaging and colony expansion of human pluripotent stem cells by enzyme-free dissociation in chemically defined culture conditions. *Nat. Protoc.* 7: 2029–2040. [Medline] [CrossRef]
3. Bernardo, A.S., Faial, T., Gardner, L., Niakan, K.K., Ortmann, D., Senner, C.E., Callery, E.M., Trotter, M.W., Hemberger, M., Smith, J.C., Bardwell, L., Moffett, A. and Pedersen, R.A. 2011. BRACHYURY and CDX2 mediate BMP-induced differentiation of human and mouse pluripotent stem cells into embryonic and extraembryonic lineages. *Cell Stem Cell* 9: 144–155. [Medline] [CrossRef]
4. Cha, J.M., Bae, H., Sadr, N., Manoucheri, S., Edalat, F., Kim, K., Kim, S.B., Kwon, I.K., Hwang, Y.S. and Khademhosseini, A. 2015. Embryoid body size-mediated differential endodermal and mesodermal differentiation using polyethylene glycol (PEG) microwell array. *Macromol. Res.* 23: 245–255. [CrossRef]
5. Chakritbudsabong, W., Sariya, L., Pamonsupornvichit, S., Pronarkngver, R., Chaiwattanarungruengpaisan, S., Ferreira, J.N., Setthawong, P., Phakdeedindan, P., Techakumphu, M., Tharasanit, T. and Rungarunlert, S. 2017. Generation of a pig induced pluripotent stem cell (piPSC) line from embryonic fibroblasts by incorporating LIN28 to the four transcriptional factor-mediated reprogramming: VSMUi001-D. *Stem Cell Res. (Amst.)* 24: 21–24. [Medline] [CrossRef]
6. Chan, K.K., Zhang, J., Chia, N.Y., Chan, Y.S., Sim, H.S., Tan, K.S., Oh, S.K., Ng, H.H. and Choo, A.B. 2009. KLF4 and PBX1 directly regulate NANOG expression in human embryonic stem cells. *Stem Cells* 27: 2114–2125. [Medline] [CrossRef]
7. Csobonyeiova, M., Polak, S., Koller, J. and Danisovic, L. 2015. Induced pluripotent stem cells and their implication for regenerative medicine. *Cell Tissue Bank.* 16: 171–180. [Medline] [CrossRef]
8. Dumont, D.J., Fong, G.H., Puri, M.C., Gradwohl, G., Alitalo, K. and Breitman, M.L. 1995. Vascularization of the mouse embryo: a study of flk-1, tek, tie, and vascular endothelial growth factor expression during development. *Dev. Dyn.* 203: 80–92. [Medline] [CrossRef]
9. Fan, J. and Watanabe, T. 2003. Transgenic rabbits as therapeutic protein bioreactors and human disease models. *Pharmacol. Ther.* 99: 261–282. [Medline] [CrossRef]
10. Ghaleb, A.M. and Yang, V.W. 2017. Krüppel-like factor 4 (KLF4): What we currently know. *Gene* 611: 27–37. [Medline] [CrossRef]
11. Greber, B., Wu, G., Bernemann, C., Joo, J.Y., Han, D.W., Ko, K., Tapia, N., Sabour, D., Sterneckert, J., Tesar, P. and Schöler, H.R. 2010. Conserved and divergent roles of FGF signaling in mouse epiblast stem cells and human embryonic stem cells. *Cell Stem Cell* 6: 215–226. [Medline] [CrossRef]
12. Hirata, H., Kawamata, S., Murakami, Y., Inoue, K., Nagahashi, A., Tosaka, M., Yoshimura, N., Miyamoto, Y., Iwasaki, H., Asahara, T. and Sawa, Y. 2007. Coexpression of platelet-derived growth factor receptor alpha and fetal liver kinase 1 enhances cardiogenic potential in embryonic stem cell differentiation in vitro. *J. Biosci. Bioeng.* 103: 412–419. [Medline] [CrossRef]
13. Hofmann, W., Schubert, D., LaBonte, J., Munson, L., Gibson, S., Scammell, J., Ferrigno, P. and Sodroski, J. 1999. Species-specific, postentry barriers to primate immunodeficiency virus infection. *J. Virol.* 73: 10020–10028. [Medline]
14. Honda, A., Hatori, M., Hirose, M., Honda, C., Izu, H., Inoue, K., Hirasawa, R., Matoba, S., Togayachi, S., Miyoshi, H. and Ogura, A. 2013. Naive-like conversion overcomes the limited differentiation capacity of induced pluripotent stem cells. *J. Biol. Chem.* 288: 26157–26166. [Medline] [CrossRef]
15. Honda, A., Hirose, M., Hatori, M., Matoba, S., Miyoshi, H., Inoue, K. and Ogura, A. 2010. Generation of induced pluripotent stem cells in rabbits: potential experimental models for human regenerative medicine. *J. Biol. Chem.* 285: 31362–31369. [Medline] [CrossRef]
16. Honsho, K., Hirose, M., Hatori, M., Yasmin, L., Izu, H., Matoba, S., Togayachi, S., Miyoshi, H., Sankai, T., Ogura, A. and Honda, A. 2015. Naïve-like conversion enhances the difference in innate in vitro differentiation capacity between rabbit ES cells and iPS cells. *J. Reprod. Dev.* 61: 13–19. [Medline] [CrossRef]
17. Hwang, Y.S., Chung, B.G., Ortmann, D., Hattori, N., Moeller, H.C. and Khademhosseini, A. 2009. Microwell-mediated control of embryoid body size regulates embryonic stem cell fate via differential expression of WNT5a and WNT11. *Proc. Natl. Acad. Sci. USA* 106: 16978–16983. [Medline] [CrossRef]
18. Ieda, M., Fu, J.D., Delgado-Olguin, P., Vedantham, V., Hayashi, Y., Bruneau, B.G. and Srivastava, D. 2010. Direct reprogramming of fibroblasts into functional cardiomyocytes by defined factors. *Cell* 142: 375–386. [Medline] [CrossRef]
19. Iida, M., Heike, T., Yoshimoto, M., Baba, S., Doi, H. and Nakahata, T. 2005. Identification of cardiac stem cells with FLK1, CD31, and VE-cadherin expression during embryonic stem cell differentiation. *FASEB J.* 19: 371–378. [Medline] [CrossRef]
20. Ikeda, Y., Collins, M.K., Radcliffe, P.A., Mitrophanous, K.A.

and Takeuchi, Y. 2002. Gene transduction efficiency in cells of different species by HIV and EIAV vectors. *Gene Ther.* 9: 932–938. [Medline] [CrossRef]

21. Kattman, S.J., Huber, T.L. and Keller, G.M. 2006. Multipotent flk-1+ cardiovascular progenitor cells give rise to the cardiomyocyte, endothelial, and vascular smooth muscle lineages. *Dev. Cell* 11: 723–732. [Medline] [CrossRef]
22. Kattman, S.J., Witty, A.D., Gagliardi, M., Dubois, N.C., Niapour, M., Hotta, A., Ellis, J. and Keller, G. 2011. Stage-specific optimization of activin/nodal and BMP signaling promotes cardiac differentiation of mouse and human pluripotent stem cell lines. *Cell Stem Cell* 8: 228–240. [Medline] [CrossRef]
23. Kehat, I., Kenyagin-Karsenti, D., Snir, M., Segev, H., Amit, M., Gepstein, A., Livne, E., Binah, O., Itskovitz-Eldor, J. and Gepstein, L. 2001. Human embryonic stem cells can differentiate into myocytes with structural and functional properties of cardiomyocytes. *J. Clin. Invest.* 108: 407–414. [Medline] [CrossRef]
24. Kopp, J.L., Ormsbee, B.D., Desler, M. and Rizzino, A. 2008. Small increases in the level of Sox2 trigger the differentiation of mouse embryonic stem cells. *Stem Cells* 26: 903–911. [Medline] [CrossRef]
25. Laflamme, M.A., Chen, K.Y., Naumova, A.V., Muskheli, V., Fugate, J.A., Dupras, S.K., Reinecke, H., Xu, C., Hassanipour, M., Police, S., O'Sullivan, C., Collins, L., Chen, Y., Minami, E., Gill, E.A., Ueno, S., Yuan, C., Gold, J. and Murry, C.E. 2007. Cardiomyocytes derived from human embryonic stem cells in pro-survival factors enhance function of infarcted rat hearts. *Nat. Biotechnol.* 25: 1015–1024. [Medline] [CrossRef]
26. Lev, S., Kehat, I. and Gepstein, L. 2005. Differentiation pathways in human embryonic stem cell-derived cardiomyocytes. *Ann. N. Y. Acad. Sci.* 1047: 50–65. [Medline] [CrossRef]
27. Levenstein, M.E., Ludwig, T.E., Xu, R.H., Llanas, R.A., VanDenHeuvel-Kramer, K., Manning, D. and Thomson, J.A. 2006. Basic fibroblast growth factor support of human embryonic stem cell self-renewal. *Stem Cells* 24: 568–574. [Medline] [CrossRef]
28. Lian, X., Hsiao, C., Wilson, G., Zhu, K., Hazeltine, L.B., Azarin, S.M., Raval, K.K., Zhang, J., Kamp, T.J. and Palecek, S.P. 2012. Robust cardiomyocyte differentiation from human pluripotent stem cells via temporal modulation of canonical Wnt signaling. *Proc. Natl. Acad. Sci. USA* 109: E1848–E1857. [Medline] [CrossRef]
29. Mohr, J.C., Zhang, J., Azarin, S.M., Soerens, A.G., de Pablo, J.J., Thomson, J.A., Lyons, G.E., Palecek, S.P. and Kamp, T.J. 2010. The microwell control of embryoid body size in order to regulate cardiac differentiation of human embryonic stem cells. *Biomaterials* 31: 1885–1893. [Medline] [CrossRef]
30. Motoike, T., Markham, D.W., Rossant, J. and Sato, T.N. 2003. Evidence for novel fate of Flk1+ progenitor: contribution to muscle lineage. *Genesis* 35: 153–159. [Medline] [CrossRef]
31. Nerbonne, J.M., Nichols, C.G., Schwarz, T.L. and Escande, D. 2001. Genetic manipulation of cardiac K(+) channel function in mice: what have we learned, and where do we go from here? *Circ. Res.* 89: 944–956. [Medline] [CrossRef]
32. Nishikawa, S.I., Nishikawa, S., Hirashima, M., Matsuyoshi, N. and Kodama, H. 1998. Progressive lineage analysis by cell sorting and culture identifies FLK1+VE-cadherin+ cells at a diverging point of endothelial and hemopoietic lineages. *Development* 125: 1747–1757. [Medline]
33. Niwa, H., Miyazaki, J. and Smith, A.G. 2000. Quantitative expression of Oct-3/4 defines differentiation, dedifferentiation or self-renewal of ES cells. *Nat. Genet.* 24: 372–376. [Medline] [CrossRef]
34. Niwa, H., Ogawa, K., Shimosato, D. and Adachi, K. 2009. A parallel circuit of LIF signalling pathways maintains pluripotency of mouse ES cells. *Nature* 460: 118–122. [Medline] [CrossRef]
35. Ogawa, M., Kizumoto, M., Nishikawa, S., Fujimoto, T., Kodama, H. and Nishikawa, S.I. 1999. Expression of alpha4-integrin defines the earliest precursor of hematopoietic cell lineage diverged from endothelial cells. *Blood* 93: 1168–1177. [Medline]
36. Osteil, P., Tapponnier, Y., Markossian, S., Godet, M., Schmaltz-Panneau, B., Jouneau, L., Cabau, C., Joly, T., Blachère, T., Gócza, E., Bernat, A., Yerle, M., Acloque, H., Hidot, S., Bosze, Z., Duranthon, V., Savatier, P. and Afanassieff, M. 2013. Induced pluripotent stem cells derived from rabbits exhibit some characteristics of naïve pluripotency. *Biol. Open* 2: 613–628. [Medline] [CrossRef]
37. Peng, X. 2012. Transgenic rabbit models for studying human cardiovascular diseases. *Comp. Med.* 62: 472–479. [Medline]
38. Pogwizd, S.M. and Bers, D.M. 2008. Rabbit models of heart disease. *Drug Discov. Today Dis. Models* 5: 185–193. [CrossRef]
39. Qian, L., Huang, Y., Spencer, C.I., Foley, A., Vedantham, V., Liu, L., Conway, S.J., Fu, J.D. and Srivastava, D. 2012. In vivo reprogramming of murine cardiac fibroblasts into induced cardiomyocytes. *Nature* 485: 593–598. [Medline] [CrossRef]
40. Ramos-Mejía, V., Montes, R., Bueno, C., Ayllón, V., Real, P.J., Rodríguez, R. and Menendez, P. 2012. Residual expression of the reprogramming factors prevents differentiation of iPSC generated from human fibroblasts and cord blood CD34+ progenitors. *PLoS One* 7: e35824. [Medline] [CrossRef]
41. Robinton, D.A. and Daley, G.Q. 2012. The promise of induced pluripotent stem cells in research and therapy. *Nature* 481: 295–305. [Medline] [CrossRef]
42. Rungarunlert, S., Klincumhom, N., Tharasanit, T., Techakumphu, M., Pirity, M.K. and Dinnyes, A. 2013. Slow turning lateral vessel bioreactor improves embryoid body formation and cardiogenic differentiation of mouse embryonic stem cells. *Cell. Reprogram.* 15: 443–458. [Medline] [CrossRef]
43. Sachinidis, A., Fleischmann, B.K., Kolossov, E., Wartenberg, M., Sauer, H. and Hescheler, J. 2003. Cardiac specific differentiation of mouse embryonic stem cells. *Cardiovasc. Res.* 58: 278–291. [Medline] [CrossRef]
44. Takahashi, K., Tanabe, K., Ohnuki, M., Narita, M., Ichisaka,

T., Tomoda, K. and Yamanaka, S. 2007. Induction of pluripotent stem cells from adult human fibroblasts by defined factors. *Cell* 131: 861–872. [Medline] [CrossRef]

45. Takei, S., Ichikawa, H., Johkura, K., Mogi, A., No, H., Yoshie, S., Tomotsune, D. and Sasaki, K. 2009. Bone morphogenetic protein-4 promotes induction of cardiomyocytes from human embryonic stem cells in serum-based embryoid body development. *Am. J. Physiol. Heart Circ. Physiol.* 296: H1793–H1803. [Medline] [CrossRef]
46. Táncos, Z., Nemes, C., Varga, E., Bock, I., Rungarunlert, S., Tharasanit, T., Techakumphu, M., Kobolák, J. and Dinnyés, A. 2017. Establishment of a rabbit induced pluripotent stem cell (RbiPSC) line using lentiviral delivery of human pluripotency factors. *Stem Cell Res. (Amst.)* 21: 16–18. [Medline] [CrossRef]
47. Thomson, M., Liu, S.J., Zou, L.N., Smith, Z., Meissner, A. and Ramanathan, S. 2011. Pluripotency factors in embryonic stem cells regulate differentiation into germ layers. *Cell* 145: 875–889. [Medline] [CrossRef]
48. van Oorschot, A.A., Smits, A.M., Pardali, E., Doevendans, P.A. and Goumans, M.J. 2011. Low oxygen tension positively influences cardiomyocyte progenitor cell function. *J. Cell. Mol. Med.* 15: 2723–2734. [Medline] [CrossRef]
49. Van Winkle, A.P., Gates, I.D. and Kallos, M.S. 2012. Mass transfer limitations in embryoid bodies during human embryonic stem cell differentiation. *Cells Tissues Organs Print* 196: 34–47. [Medline] [CrossRef]
50. Yang, L., Soonpaa, M.H., Adler, E.D., Roepke, T.K., Kattman, S.J., Kennedy, M., Henckaerts, E., Bonham, K., Abbott, G.W., Linden, R.M., Field, L.J. and Keller, G.M. 2008. Human cardiovascular progenitor cells develop from a KDR+ embryonic-stem-cell-derived population. *Nature* 453: 524–528. [Medline] [CrossRef]
51. Zhang, J., Klos, M., Wilson, G.F., Herman, A.M., Lian, X., Raval, K.K., Barron, M.R., Hou, L., Soerens, A.G., Yu, J., Palecek, S.P., Lyons, G.E., Thomson, J.A., Herron, T.J., Jalife, J. and Kamp, T.J. 2012. Extracellular matrix promotes highly efficient cardiac differentiation of human pluripotent stem cells: the matrix sandwich method. *Circ. Res.* 111: 1125–1136. [Medline] [CrossRef]